TITLE

Solution structure of the *E. coli* TolA C–terminal domain reveals induced fit by the binding of the phage minor coat gene 3 protein N–terminal domain.

INTRODUCTION

The Tol-Pal system of *Escherichia coli* is composed of two protein complexes located in the cell envelope. One is located in the cytoplasmic membrane and involves the TolA, TolQ and TolR proteins interacting with each other by their transmembrane segments (Derouiche *et al.*, 1995; Lazzaroni *et al.*, 1995). The other complex is associated with the outer membrane (Bouveret *et al.*, 1995) and is composed of the outer membrane anchored Pal lipoprotein and the periplasmic TolB protein. Cross-talk between the two complexes was recently detected. TolA interacts with Pal and this interaction requires the proton motive force {Cascales, Gavioli, *et al.* 2000 #78} and the TolQ, TolR protéins {Cascales, Lloubès, *et al.* 2001 #601}. TolA also interacts with the N–terminal domain of TolB {Walburger, Lazdunski, *et al.* 2002 #531}. The precise function of the Tol-Pal system remains unknown apart from its role in cell envelope integrity (Lloubès *et al.*, 2001). A pleiotropic phenotype linked to the loss of outer membrane integrity has been observed for *tol* and *pal* mutants which are leaky for periplasmic proteins, hypersensitive to drugs and detergents (Levengood *et al.*, 1993), and release outer membrane vesicles (Bernadac *et al.*, 1998).

Phylogenetic studies have shown that the *tol-pal* gene cluster was well conserved throughout the Eubacteria (Sturgis, 2001). In *Vibrio cholerae*, *tolQRA* genes are required for the import of cholera toxin (Heilpern and Waldor, 2000). In *Pseudomonas aeruginosa*, *tolA* is one of the 34 genes activated in biofilm populations, which are resistant to antimicrobial treatment (Whiteley *et al.*, 2001).

The Tol-Pal system of *Escherichia coli* is parasitized by group A colicins (bacterial toxins produced by and active against *E. coli* and closely related bacteria, {Bénédetti & Géli 1996 #38}) and filamentous single-stranded DNA bacteriophages (Webster, 1991). Infection by filamentous bacteriophages is mediated by the g3p protein, a minor coat protein located at the end of the phage capsid. The g3p protein has a modular structure composed of three domains (N1, N2 and CT) separated by glycine-rich linkers and in addition a short C-terminal transmembrane segment. The three-dimensional structure of the two N-terminal domains of g3p from phage M13 and fd has been solved (Lubkowski *et al.*, 1998), (Holliger *et al.*, 1999).

According to the current model, infection of the host cells is initiated by binding of the g3p central domain to the tip of a F-pilus which is presumably then retracted, thereby guiding the bound phage to the cell envelope. At this stage the interaction of the g3p N-terminal domain with the TolA protein would trigger an as yet unknown process leading to the entry of the phage DNA into the bacterial cytoplasm (Riechmann and Holliger, 1997), (Click and Webster, 1998).

The TolA protein consists of three domains {Levengood, Beyer, *et al.* 1991 #59}. The N-terminal domain (residues 1 to 47) which anchors the protein in the cytoplasmic membrane, the central domain (residues 48 to 310) which is assumed to be an α-helical structure long enough to span the periplasmic space, and the C–terminal domain (residues 311 to 421) involved in the interaction with group A colicins (for a review see (Lazdunski *et al.*, 1998) and with the minor coat g3p protein.

The only tridimensional structure of the C–terminal domain of *Escherichia coli* TolA (TolAIII) available until now was the X–ray structure of a fused protein comprising the N–terminal domain of g3p (g3p N1) and TolAIII (Lubkowski *et al.*, 1999). In this structure, g3p N1 was shown to interact closely to the first helix of TolAIII and to its last ß strand, which extends the g3p N1 ß sheet.

We have shown in our previous work on free TolAIII (Deprez *et al.*, 2002) that the secondary structure elements are conserved in the free and complexed forms of TolAIII. However, we observed that the ^{15}N–^{1}H HSQC spectrum of TolAIII was highly altered by the binding of g3p N1, as all resonances shift in the NMR spectrum. Usually, binding only affects the resonances at the protein-protein interface. This is the basis of chemical shift perturbation mapping (Zuiderweg, 2002). Therefore, these results suggest that the binding of g3p N1 might induce conformational changes in TolAIII.

In an attempt to clarify this point, we solved the solution structure of free TolAIII by NMR spectroscopy. We compare this structure with the crystal structure of TolAIII in complex with g3p N1, as well as with the crystal structure of the C–terminal domain of *Pseudomonas aeruginosa* TolA, which was solved recently (Witty *et al.*, 2002).

RESULTS

Solution structure determination

We have determined the structure of the free TolAIII3 domain in solution using heteronuclear double and triple resonance NMR spectroscopy. Assignment of ^{1}H, ^{13}C and ^{15}N chemical shifts was determined previously (Deprez *et al.*, 2000). 50 couples of (Φ,Ψ) backbone torsion angles were derived from these assignments using the program TALOS (Cornilescu *et al.*, 1999).

The structure was calculated with a two-step semi-automated procedure using ARIA 1.0 (Nilges and O'Donoghue, 1998). In a first structure calculation step, 587 manually assigned distance restraints from the ^{15}N 3D-NOESY-HSQC and ^{13}C 3D-NOESY-HSQC experiments were used, as well as 198 unassigned distance restraints from a 2D-NOESY experiment, 100 backbone torsion angles and 18 hydrogen bonds in canonical alpha helices based on secondary structure elements determined previously (Deprez *et al.*, 2002). In the second step starting from the 10 lowest energy structures from the first step, the 100 backbone torsion angles and all available (assigned or unassigned) distance restraints from the three NOESY experiments were used, resulting in 724 unambiguous and 125 ambiguous distance restraints generated in the last iteration of ARIA. 68 restraints were rejected because they led to systematic violations higher than 0.1 Å. The distribution of the 724 (non redundant) unambiguous distance restraints obtained after merging of the data in the last iteration is shown in figure 1. Analysis of the 16 best structures (regarding total energy) from the last iteration shows that no distance violation higher than 0.1 Å are present in more than 3 structures and that no dihedral restraint is violated by more than 8°. This structural ensemble was water refined using the standard protocol of ARIA 1.2. Structural statistics are shown in table 1. The circular variances (MacArthur and Thornton, 1993) of phi and psi angles (figure 2) indicate a higher variability in dihedrals for residues 1 to 15 and 30 to 39. Residues in disallowed regions of the Ramachandran plot are located exclusively in these regions.

Comparison between the structure of free TolAIII and that of TolAIII complexed to g3p N1

The general fold of free TolAIII is the same as that of TolAIII complexed to g3p.

The poor definition of residues 1 to 15 is confirmed by the high mobility observed from N–H heteronuclear NOEs in this region (Deprez *et al.*, 2002) and by the structural disorder

which made this region unobservable in the crystal structure of TolAIII-g3p (Lubkowski *et al.*, 1999).

The structure of residues 30 to 40 (including 1 glycine, 2 serine and 2 alanine residues) is not well defined either. However, it is unclear at first if this is due only to a lack of experimental distance restraints in this wide loop or if it is due to mobility (the lack of experimental restraints being accounted for by mobility). Nevertheless, N–H heteronuclear NOEs measured in this region indicate a certain mobility, whereas in the crystal structure of TolAIII-g3p, this region is well defined according to b factors.

On the contrary, the alpha helix between residues 15 and 30 of free TolAIII is well defined relatively to the rest of the protein, owing to several unambiguous long-range distance restraints (figure 3). This α-helix participates to the binding site of g3p, along with the last ß strand of TolAIII. This well-defined region appears to undergo significant conformational changes due to the binding of g3p (figure 4). In fact, when the ß strand ß4 of g3p and the last ß strand of TolAIII (Leu96 to Lys99) are put together as in the crystal structure of the complex, Tyr54 of g3p-N1 overlaps Asn17 of TolAIII and Val43 of g3p-N1 overlaps Lys24. On the contrary, when the helix is shifted forwards along its axe by nearly one turn, as in the crystal structure, Lys24 is replaced by Glu28, replaces Gly21 and forms a hydrophilic pocket with the side chain of ThrA56 and the carboxyl of ThrA41 and ValA43. As well, Asn17 is replaced by Ala20 and forms a hydrogen bond with SerA16. Inside the hydrophobic core of TolAIII, Phe31 takes the place of Ile27, Ile27 takes the place of Ile23, Ile23 takes the place of Tyr19. In the end, the poor definition of the loop between residues 30 and 40 of TolAIII may be related to the shifting of the first alpha helix of TolAIII in order to accomodate for g3p binding.

The loop and helix between residues Ala77 and Phe91 are shifted along with the first helix as hydrophobic contacts are conserved associating Ile16 with Val87 and Val90, Tyr19 with Phe91, Ile23 with Ile79, and Ala26 with Ala77.

The tertiary structure of the ß sheet of TolAIII is altered by the interaction with g3p (figure 4). In free TolAIII, the bulge created by residues Pro59 and Glu60 in the ß strand from Leu54 to Gly62 breaks the ß sheet into two parts, inducing a severe torsion. When binding with g3p, the ß sheet stretches and the last ß strand of TolAIII is extended, as Pro95 and Arg45 flip and the carboxyl group of Leu96 points toward the amide group of Cys46 of g3p. A difference of 38° ± 8° is observed for the Φ angle of Leu96 between the free and the complexed form of g3p.

Comparison with the structure of free *Pseudomonas aeruginosa* TolAIII

Although the sequence similarity between *E. coli* and *P. aeruginosa* TolAIII is only 20%, the fold is very similar between the two domains.

With the same alignment of the last ß strand (residues Ile114 to Lys117 in *P. aeruginosa* and residues Leu96 to Lys99 in *E. coli*) as above, the ß strand in free *P. aeruginosa* TolAIII appears even more bended than in free *E. coli* TolAIII, whereas the first α helix is in an intermediate position between those of free and g3p-complexed *E. coli* TolAIII.

Interestingly, the loop between the first α helix and the first ß strand, which was found poorly defined in the NMR structure, shows no apparent structural similarity either between the X-ray structures of *P. aeruginosa* TolAIII and of *E. coli* TolAIII-g3p N1.

EXPERIMENTAL PROCEDURES

Sample Preparation

Isotopically ^{15}N-labeled and ^{15}N/^{13}C double-labeled samples of TolA (accession number swiss-prot P19934) spanning amino acids 325 to 421 (corresponding respectively to residue 4 and 100 in our numbering scheme) were obtained from bacteria grown in M9 minimal medium containing respectively 1 g/L $^{15}NH_4Cl$, and 1 g/L $^{15}NH_4Cl$ and 2 g/L $^{13}C_6$-Glucose as sole nitrogen and carbon sources. The protein was overexpressed in the periplasm of *E. coli* strain BL21. The construct contained 3 additional residues (AEF) at the N-terminus of the mature protein and 6 additional histidine residues at the C-terminus for purification purpose, which were not removed. Details on the expression and purification were published elsewhere (Deprez *et al.*, 2002).

NMR Spectroscopy

Interproton distance restraints were derived from three NMR experiments acquired at 300 K, in 90% H_2O/10% D_2O, with a NOE mixing time of 0.08 s, on a Varian Inova spectrometer (800 MHz) equipped with a triple resonance (^{1}H, ^{13}C, ^{15}N) probe including shielded z-gradients. All triple resonance experiments used the pulse sequences provided by the Varian protein pack (available at ftp site : ftp.nmr.varian.com). All data were processed with Felix (Accelrys Inc.) using 90° shifted sine-bell squared apodizing functions. Residual water suppression was achieved using a sinebell convolution.

A homonuclear 2D-NOESY experiment was recorded on a 1.4 mM sample of ^{15}N labeled TolAIII3 in 100 mM NaCl, 50 mM $NaPO_4$ (pH 6.8) with digital resolutions of 4.9 Hz or 0.006 ppm (^{1}H direct dimension) and 27.7 Hz or 0.035 ppm (^{1}H indirect dimension). A first order polynomial baseline correction was applied in the direct dimension.

A heteronuclear ^{13}C 3D-NOESY-HSQC experiment was recorded on a 0.5 mM sample of ^{15}N/^{13}C doubly labeled TolAIII3 in 50 mM NaCl, 50 mM $NaPO_4$ (pH 6.8) as well as protease inhibitor cocktail (Complete, Boehringer Mannheim) with digital resolutions of 11.7 Hz or 0.015 ppm (^{1}H direct dimension), 78.1 Hz or 0.098 ppm (^{1}H indirect dimension) and 106.2 Hz or 0.133 ppm (^{13}C indirect dimension). A second order polynomial baseline correction was applied in the ^{1}H indirect dimension.

A heteronuclear ^{15}N 3D-NOESY-HSQC experiment was recorded on a 0.7 mM sample of ^{15}N labeled TolAIII3 in 500 mM NaCl, 50 mM $NaPO_4$ (pH 6.8) with digital resolutions of

9.8 Hz or 0.012 ppm (^{1}H direct dimension), 40 Hz or 0.05 ppm (^{1}H indirect dimension) and 55.6 Hz or 0.069 ppm (^{15}N indirect dimension).

Peak Picking and Manual Assignment of nOe Cross Peaks

Using the 2D-NOESY experiment, an automatic peak-picking of all predicted intraresidual correlations, based on the chemical shift table, was displayed. Calibration was adjusted consequently and 198 new (interresidual) peaks were picked manually in the aliphatic region (0.0 to 5.5 ppm) by examining both sides of the diagonal to take advantage of the better resolution in the direct dimension.

Using the ^{13}C 3D-NOESY-HSQC experiment, an automatic peak-picking of all predicted intraresidual correlations, based on the chemical shift table, was displayed. Calibration was adjusted consequently. 319 new (interresidual) peaks were picked manually and compared to the chemical shift table with a deviation of +/- 0.03 ppm to provide virtual assignments automatically. All 87 peaks with an assignment ambiguity lower than 5 were examined. Ambiguity could be reduced for 55 of them according to misalignments in the spectrum. 264 correlations remained unassigned.

Using the ^{15}N 3D-NOESY-HSQC experiment, an automatic peak-picking of all predicted intraresidual and sequential correlations, based on the chemical shift table, was displayed. Picked peaks were adjusted, merged or removed when necessary, resulting in 497 intraresidual and sequential distance restraints. 91 new peaks were picked, among which 27 were assigned manually based on secondary structure elements (18 H_A^{i}/H_N^{i+3} distance restraints in α-helices and 9 inter-ß-strand distance restraints). Unassigned correlations were compared to the chemical shift table with a deviation of +/- 0.02 ppm to provide virtual assignments automatically. All 35 peaks with an assignment ambiguity lower than 5 were examined. Ambiguity could be reduced for 8 of them according to misalignments in the spectrum. 56 correlations remained unassigned.

Structure Calculation

The structure of the free TolAIII3 domain in solution was calculated in a two-step semi-automated procedure using ARIA 1.0 (Nilges and O'Donoghue, 1998). In all calculations, a disulfide bridge was formed between cysteine residues 42 and 67, according to previous mass spectroscopy data (Deprez *et al.*, 2002) and to the high chemical shifts of the $C_ß$ of cysteine residues 42 and 67 (48.7 and 37.6 ppm respectively). ARIA standard distance calibration were used.

In a first step, a run was launched from randomized initial coordinates using the assigned data from both ^{15}N and ^{13}C 3D-NOESY HSQC experiments and the unassigned peak list from the 2D-NOESY experiment (PPMDPRO1=0.015 and PPMDPRO2=0.03) as well as 100 backbone torsion angles and 18 hydrogen bonds in canonical alpha helices based on secondary structure elements determined previously (Deprez *et al.*, 2002). Standard parameters were used except that 80 structures were calculated in iteration 0 and 160 in iteration 8. The run was reproduced with 150 structures in all iterations and the 10 best structures regarding the nOe energy were selected for the second step. Backbone RMSD calculated for residues 15 to 100 was 1.879 Å for this ensemble. Distance restraint violations were inspected and peak-pickings corrected when necessary. As residues 27 to 40 and 98 to 101 were poorly defined, additional distance restraints were searched for manually, resulting in 54 new restraints in the ^{13}C 3D-NOESY HSQC in the end.

In the second step, a run was launched from the 10 structures conserved previously (filling iteration 0). All available nOe data (unassigned or assigned, ambiguous or not) were used, as well as the but without hydrogen bonds. Assigned distance restraints were weighted (>1), which means that they could not be rejected during the process. On the contrary, unassigned distance restraints could be rejected if they were systematically violated. Unassigned distance restraints were iteratively processed by ARIA (parameters given in tables 2 and 3) and progressively assigned automatically.

Coordinate precision[1]	
RMSD c, ca, n (Å)	0.973 ± 0.139
RMSD heavy atoms (Å)	1.530 ± 0.181
Experimental restraints	
NOE Distances (Å)	0.022 ± 0.007
Dihedral angles (deg)	0.446 ± 0.183
Geometry analysis	
Bonds (Å)	0.003 ± 0.0001
Angles (deg)	0.440 ± 0.020
Impropers (deg)	1.255 ± 0.100
Ramachandran analysis (PROCHECK)	
Residues in most favoured regions (%)	80.31
Residues in additional allowed regions (%)	16.20
Residues in generously allowed regions (%)	1.56
Residues in disallowed regions (%)	1.93

Table 1 : Structural Statistics for the 16 lowest energy structures from the last iteration, refined in water

[1] calculated over residues 15 to 100.

ARIA Parameter	^{15}N edited NOESY-HSQC	^{13}C edited NOESY-HSQC	homonuclear NOESY-HSQC
PPMDHET1	± 0.4	± 0.4	-
PPMDPRO1	± 0.03	± 0.03	± 0.015
PPMDPRO2	± 0.02	± 0.03	± 0.03

Table 2 : Chemical shift tolerances (ppm) used for the ARIA automated processing of unassigned peaks in the second step of the structure calculation (file new.html)

iteration	structures calculated	assignment cutoff	violation threshold
0	80	0.9	1.0
1	80	0.9	1.0
2	80	0.9	0.5
3	80	0.85	0.3
4	80	0.82	0.2
5	80	0.8	0.3
6	80	0.8	0.2
7	80	0.8	0.1
8	1000	0.8	0.1

Table 3 : Non-standard parameters used in the ARIA iterations in the second step of the structure calculation (file run.cns). Besides, 15 structures were kept from one iteration onto the next one.

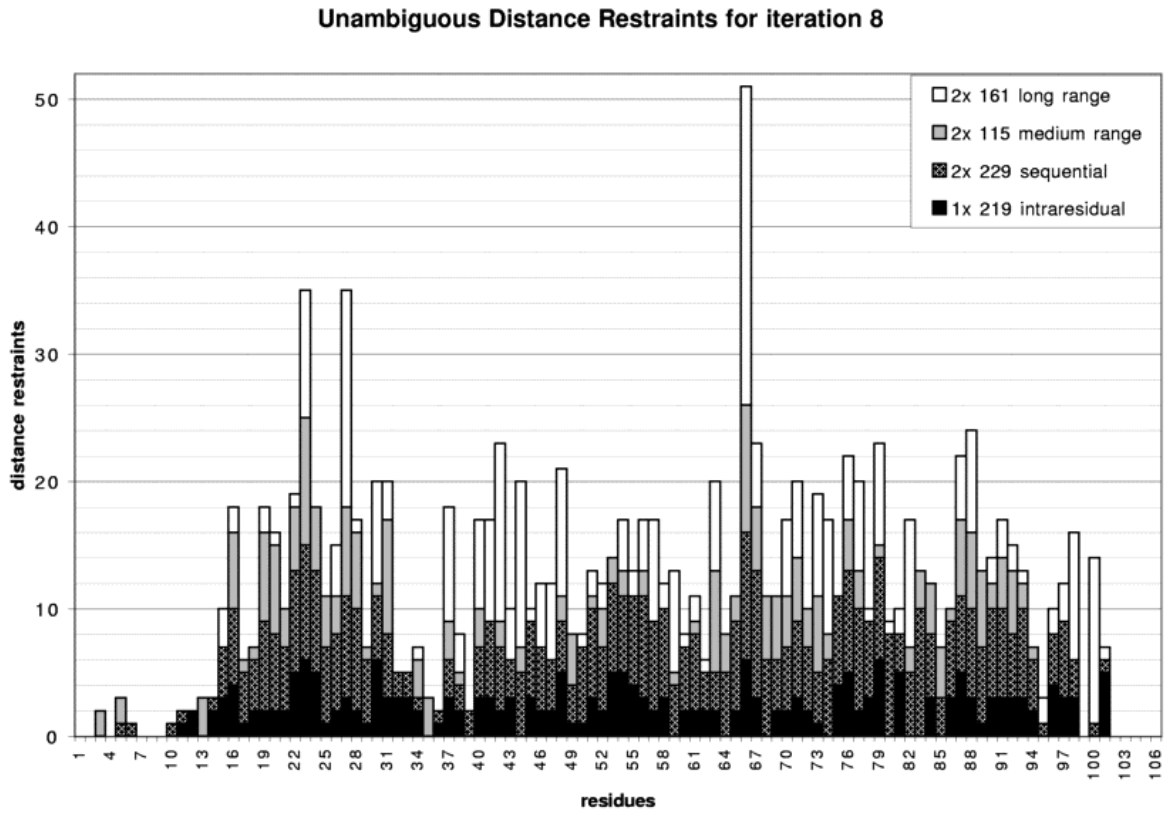

Figure 1 : Distribution of the 724 unambiguous distance restraints obtained after merging of the data in the last ARIA iteration of the second step of the structure calculation. Restraints are classified as intraresidue (i-j=0), sequential (|i-j|=1), medium range (|i-j|<5) and long range (|i-j|>4) NOEs. The 125 ambiguous distance restraints are not shown.

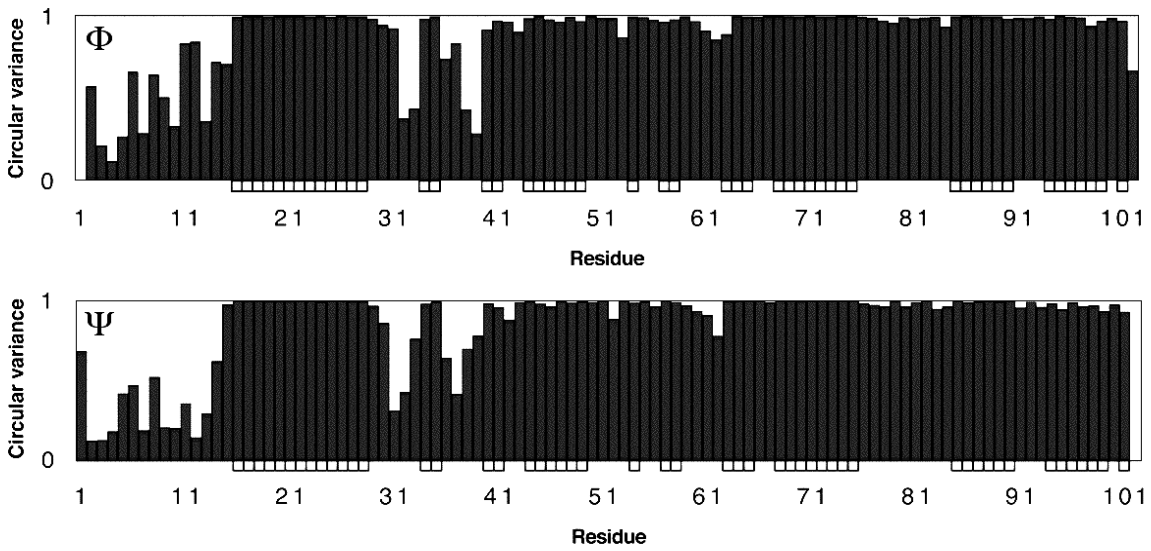

Figure 2 : Circular variance for angle Φ (top) and Ψ (bottom), calculated on the 16 water-refined lowest energy structures. Small squares indicate TALOS derived dihedral restraints used in the calculations.

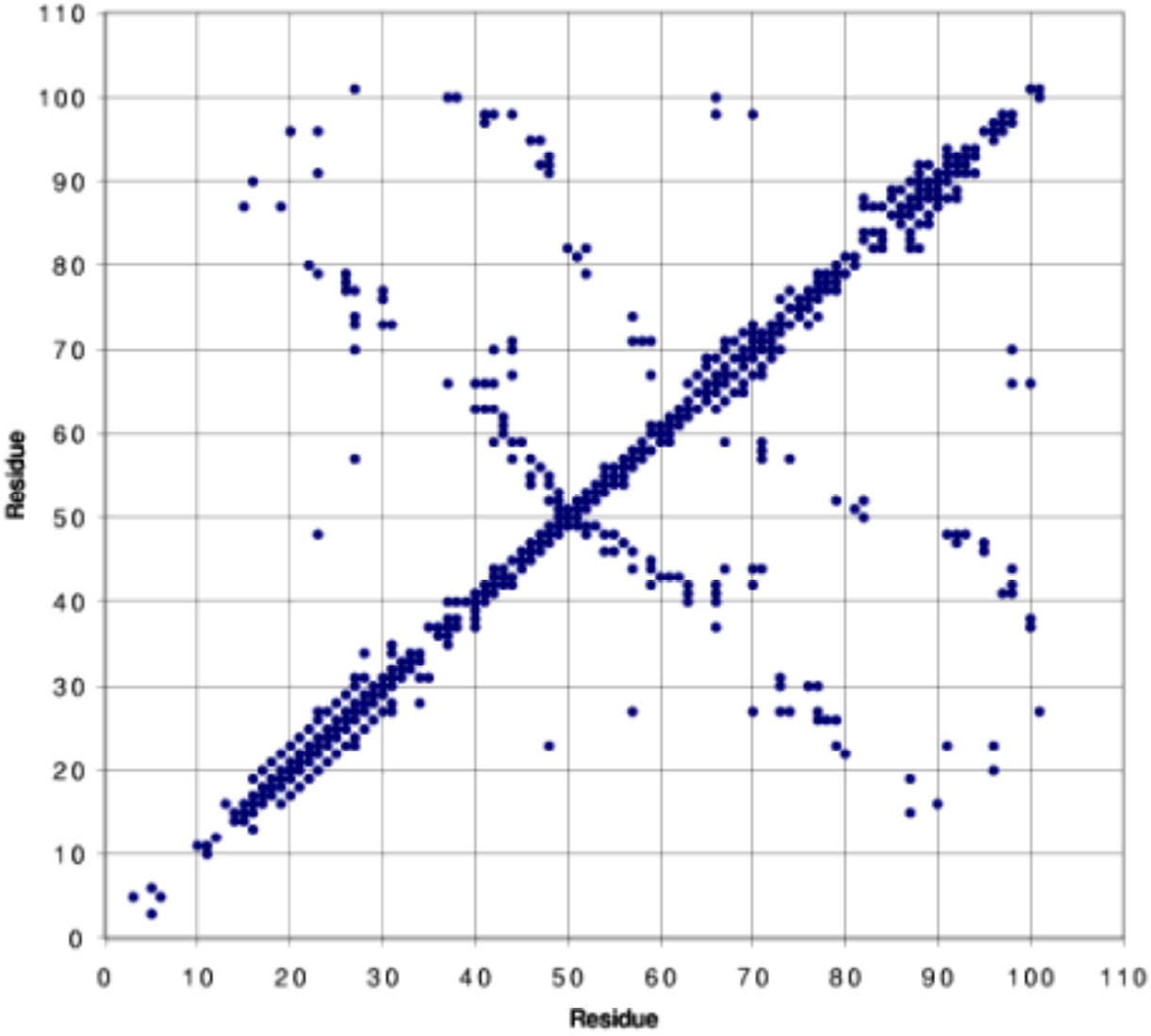

Figure 3 : Contact map for unambiguous distance restraints after merging of the data in the last ARIA iteration of the second step of the structure calculation.

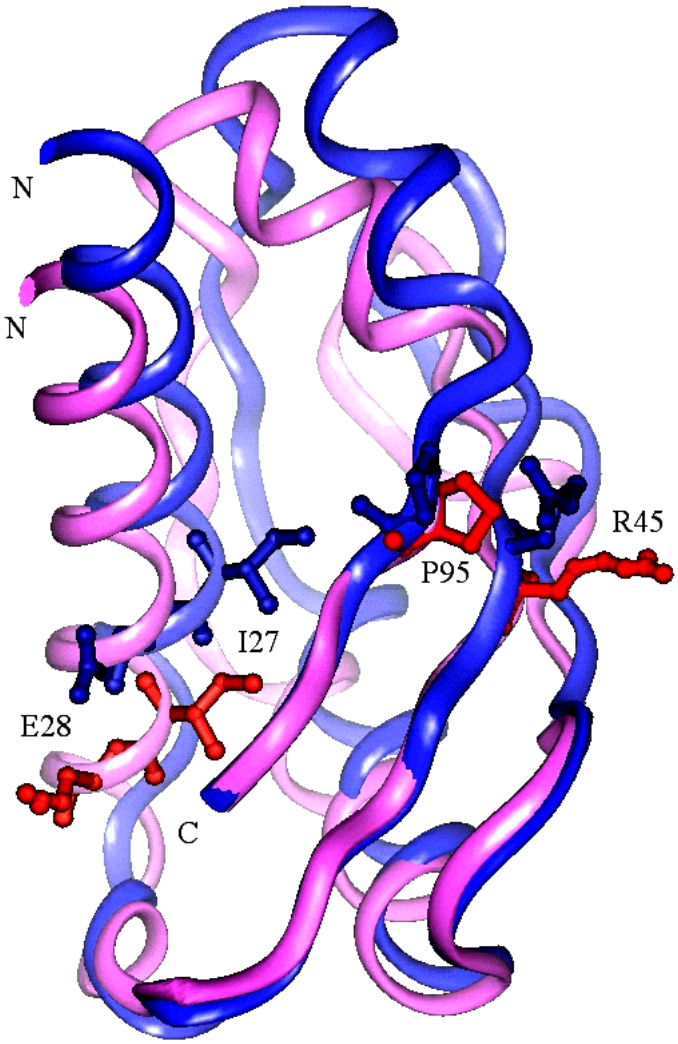

Figure 4 : Ribbon representation of the backbone structure of free TolAIII (red : averaged over the 16 lowest energy NMR structures) and of TolAIII when bound to g3p N1 (blue : extracted form the TolAIII–g3p N1 crystal structure).
Residues Ile27, Glu28, Arg45 and Pro95 are highlighted in both structures.
Structures were superimposed along the backbone atoms (c, ca, n, o) of the part of the ß sheet interacting with g3p N1 in the structure of the complex (residues 42 to 43, 60 to 61, 96 to 99).
The figure was created with Insight (Accelrys)

REFERENCES

Bernadac, A., Gavioli, M., Lazzaroni, J.C., Raina, S., and Lloubès, R. (1998) *Escherichia coli tol-pal* Mutants Form Outer Membrane Vesicles *Journal of Bacteriology* **180(18)**: 4872-4878.

Bouveret, E., Derouiche, R., Rigal, A., Lloubès, R., Lazdunski, C., and Benedetti, H. (1995) Peptidoglycan-associated lipoprotein-TolB interaction. A possible key to explaining the formation of contact sites between the inner and outer membranes of Escherichia coli. *J Biol Chem* **270**: 11071-7.

Click, E. M. and Webster, R. E. (98) The TolQRA proteins are required for membrane insertion of the major capsid protein of the filamentous phage f1 during infection. *J Bacteriol* **180**: 1723-8.

Cornilescu, G., Delaglio, F., and Bax, A. (99) Protein backbone angle restraints from searching a database for chemical shift and sequence homology. *J Biomol NMR* **13**: 289-302.

Deprez, C., Blanchard, L., Guerlesquin, F., Gavioli, M., Simorre, J.-P., Lazdunski, C., Marion, D., and Lloubès, R. (2002) Macromolecular Import into Escherichia coli: The TolA C-Terminal Domain Changes Conformation When Interacting with the Colicin A Toxin *Biochemistry* **41**: 2589-2598.

Deprez, C., Blanchard, L., Simorre, J.P., Gavioli, M., Guerlesquin, F., Lazdunski, C., Lloubès, R., and Marion, D. (2000) Assignment of the 1H, 15N and 13C resonances of the C-terminal domain of the TolA protein of Escherichia coli, involved in cell envelope integrity. *J Biomol NMR* **18**: 179-80.

Derouiche, R., Bénédetti, H., Lazzaroni, J.C., Lazdunski, C., and Lloubès, R. (1995) Protein Complex within *Escherichia coli* Inner Membrane *The Journal of Biological Chemistry* **270(19)**: 11078-11084.

Heilpern, A.J. and Waldor, M.K. (2000) CTXphi infection of Vibrio cholerae requires the tolQRA gene products. *J Bacteriol* **182**: 1739-47.

Holliger, P., Riechmann, L., and Williams, R.L. (1999) Crystal Structure of the Two N-terminal Domains of g3p from Filamentous Phage fd at 1.9 A : Evidence for Conformational Lability *J.Mol.Biol.* **288**: 649-657.

Lazdunski, C., Bouveret, E., Rigal, A., Journet, L., Lloubès, R., and Bénédetti, H. (1998) Colicin Import into *Escherichia coli* Cells *Journal of Bacteriology* **180(19)**: 4993-5003.

Lazzaroni, J.C., Vianney, A., Popot, J.L., Bénédetti, H., Samatey, F., Lazdunski, C., Portalier, R., and Géli, V. (1995) Transmembrane α-Helix Interactions are Required for the Functional Assembly of the *Escherichia coli* Tol Complex *J.Mol.Biol.* **246**: 1-7.

Levengood, S.K., Click, E.M., and Webster, R.E. (1993) Role of the Carboxyl-Terminal Domain of TolA in Protein Import and Integrity of the Outer Membrane *Journal of Bacteriology* **175(1)**: 222-228.

Lloubès, R., Cascales, E., Walburger, A., Bouveret, E., Lazdunski, C., Bernadac, A., and Journet, L. (2001) The Tol-Pal proteins of the Escherichia coli cell envelope: an energized system required for outer membrane integrity? *Res Microbiol* **152**: 523-9.

Lubkowski, J., Hennecke, F., Plückthun, A., and Wlodawer, A. (1998) The structural basis of phage display elucidated by the crystal structure of the N-terminal domains of g3p *nature structural biology* **5(2)**: 140-147.

Lubkowski, J., Hennecke, F., Plückthun, A., and Wlodawer, A. (1999) Filamentous phage infection : crystal structure of g3p in complex with its coreceptor, the C-terminal domain of TolA *Structure* **7(6)**: 711-722.

MacArthur, M. W. and Thornton, J. M. (93) Conformational analysis of protein structures derived from NMR data. *Proteins* **17**: 232-51.

Nilges, M. and O'Donoghue, S. I. (98) Ambiguous NOEs and automated NOE assignment. *Progress in Nuclear Magnetic Resonance Spectroscopy* **32**: 107-139.

Riechmann, L. and Holliger, P. (1997) The C-Terminal Domain of TolA Is the Coreceptor for Filamentous Phage Infection of E. coli *Cell* **90**: 351-360.

Sturgis, J.N. (2001) Organisation and evolution of the tol-pal gene cluster. *J Mol Microbiol Biotechnol* **3**: 113-22.

Webster, R.E. (1991) The *tol* gene and the import of macromolecules into *Escherichia coli Molecular Microbiology* **5(5)**: 1005-1011.

Whiteley, M., Bangera, M.G., Bumgarner, R.E., Parsek, M.R., Teitzel, G.M., Lory, S., and Greenberg, E.P. (2001) Gene expression in Pseudomonas aeruginosa biofilms. *Nature* **413**: 860-4.

Witty, M., Sanz, C., Shah, A., Grossmann, J. G., Mizuguchi, K., Perham, R. N., and Luisi, B. (2002) Structure of the periplasmic domain of Pseudomonas aeruginosa TolA: evidence for an evolutionary relationship with the TonB transporter protein. *EMBO J* **21**: 4207-18.

Zuiderweg, E. R. (2002) Mapping protein-protein interactions in solution by NMR spectroscopy. *Biochemistry* **41**: 1-7.